J. Math. Sci. Univ. Tokyo
24 (2017), 399–430.

Abundance of Nilpotent Orbits in Real Semisimple Lie Algebras

By Takayuki Okuda

Abstract. We formulate and prove that nilpotent orbits are "abundant" in real semisimple Lie algebras, in the following sense. If S denotes the collection of hyperbolic elements corresponding the weighted Dynkin diagrams coming from nilpotent orbits, then S spans the maximally expected space, namely, the (-1)-eigenspace of the longest Weyl group element. The result is used to the study of fundamental groups of non-Riemannian locally symmetric spaces.

1. Main Theorem

Let $\mathfrak{g}$ be a real semisimple Lie algebra, $\mathfrak{a}$ a maximally split abelian subspace of $\mathfrak{g}$, and W the Weyl group of $\Sigma(\mathfrak{g},\mathfrak{a})$. We fix a positive system $\Sigma^+(\mathfrak{g},\mathfrak{a})$, denote by $\mathfrak{a}_+(\subset\mathfrak{a})$ the closed Weyl chamber, w_0 the longest element of W, and set $\mathfrak{a}^{-w_0}:=\{A\in\mathfrak{a}\mid -w_0\cdot A=A\}$.

We denote by $\mathrm{Hom}(\mathfrak{sl}(2,\mathbb{R}),\mathfrak{g})$ the set of all Lie algebra homomorphisms from $\mathfrak{sl}(2,\mathbb{R})$ to $\mathfrak{g}$, and put

$$\mathcal{H}^n(\mathfrak{g}):=\left\{\rho\begin{pmatrix}1&0\\0&-1\end{pmatrix}\in\mathfrak{g}\;\middle|\;\rho\in\mathrm{Hom}(\mathfrak{sl}(2,\mathbb{R}),\mathfrak{g})\right\},$$
$$\mathcal{H}^n(\mathfrak{a}_+):=\mathfrak{a}_+\cap\mathcal{H}^n(\mathfrak{g}).$$

In this paper, we prove the following theorem:

Theorem 1.1. $\mathfrak{a}^{-w_0}=\mathbb{R}\text{-span}(\mathcal{H}^n(\mathfrak{a}_+))$.

In Theorem 1.1, the inclusion

$$\mathfrak{a}^{-w_0}\subset\mathbb{R}\text{-span}(\mathcal{H}^n(\mathfrak{a}_+)) \tag{1.1}$$

2010 *Mathematics Subject Classification.* Primary 17B08; Secondary 57S30.
Key words: Nilpotent orbit, weighted Dynkin diagram, Satake diagram, Dynkin–Kostant classification.

is non-trivial and the opposite inclusion is easy (see Section 3 for more details).

Theorem 1.1 means that nilpotent orbits are "abundant" in $\mathfrak{g}$ in the following sense (see (1.2)). Let us denote by $\mathcal{N}(\mathfrak{g})$ the set of all nilpotent elements in $\mathfrak{g}$. Then by results of Jacobson–Morozov and Kostant, we have

$$\mathcal{N}(\mathfrak{g}) = \left\{ \rho \begin{pmatrix} 0 & 1 \\ 0 & 0 \end{pmatrix} \in \mathfrak{g} \;\middle|\; \rho \in \mathrm{Hom}(\mathfrak{sl}(2,\mathbb{R}), \mathfrak{g}) \right\}$$

and for each nilpotent (adjoint) orbit $\mathcal{O} \in \mathcal{N}(\mathfrak{g})/\mathrm{Int}\,\mathfrak{g}$, there exists a unique $A_{\mathcal{O}} \in \mathcal{H}^n(\mathfrak{a}_+)$ such that $\rho \begin{pmatrix} 1 & 0 \\ 0 & -1 \end{pmatrix} = A_{\mathcal{O}}$ and $\rho \begin{pmatrix} 0 & 1 \\ 0 & 0 \end{pmatrix} \in \mathcal{O}$ for some $\rho \in \mathrm{Hom}(\mathfrak{sl}(2,\mathbb{R}), \mathfrak{g})$ (see [4, Section 9.2] for more details). Then the correspondence $\mathcal{O} \mapsto A_{\mathcal{O}}$ gives a surjective map:

$$\phi : \mathcal{N}(\mathfrak{g})/\mathrm{Int}\,\mathfrak{g} \twoheadrightarrow \mathcal{H}^n(\mathfrak{a}_+).$$

The non-trivial part (1.1) of Theorem 1.1 is equivalent to the following inclusion:

$$\mathfrak{a}^{-w_0} \subset \mathbb{R}\text{-span}\ \phi(\mathcal{N}(\mathfrak{g})/\mathrm{Int}\,\mathfrak{g}). \tag{1.2}$$

Theorem 1.1 was announced in [9, Proposition 4.8 (i)]. More precisely, Theorem 1.1 played a key role in proving one of the main results in [9] which claims that semisimple symmetric spaces G/H admit properly discontinuous groups which are not virtually-abelian if and only if G/H admit proper actions of $SL(2,\mathbb{R})$ (see also Appendix A). We illustrated an idea of the proof in [9, Section 7.5] by an example $\mathfrak{g} = \mathfrak{su}(4,2)$, but postponed a full proof to this paper.

2. Algorithm to Classify Hyperbolic Elements Coming from Nilpotent Orbits

In this section, we recall the algorithm to classify elements in $\mathfrak{a}^{-w_0}$ and $\mathcal{H}^n(\mathfrak{a}_+)$ described in [9].

2.1. Notation

We set up our notation. Let $\mathfrak{g}_{\mathbb{C}}$ be a complex semisimple Lie algebra and $\mathfrak{g}$ a real form of $\mathfrak{g}_{\mathbb{C}}$. We fix a Cartan decomposition $\mathfrak{g} = \mathfrak{k} + \mathfrak{p}$ with a Cartan involution θ on $\mathfrak{g}$.

Take a θ-stable split Cartan subalgebra $\mathfrak{j}_0$ of $\mathfrak{g}$. That is, $\mathfrak{j}_0$ is a maximal abelian subspace of $\mathfrak{g}$ stable by θ such that $\mathfrak{a} := \mathfrak{j}_0 \cap \mathfrak{p}$ is a maximal abelian subspace of $\mathfrak{p}$. Then $\mathfrak{j}_0$ can be written as $\mathfrak{j}_0 = \mathfrak{t} + \mathfrak{a}$ where $\mathfrak{t}$ is a maximal abelian subspace of the centralizer $Z_{\mathfrak{k}}(\mathfrak{a})$ of $\mathfrak{a}$ in $\mathfrak{k}$. Let us denote by $\mathfrak{j}_{\mathbb{C}} := \mathfrak{j}_0 + \sqrt{-1}\mathfrak{j}_0$ and $\mathfrak{j} := \sqrt{-1}\mathfrak{t} + \mathfrak{a}$. Then $\mathfrak{j}_{\mathbb{C}}$ is a Cartan subalgebra of $\mathfrak{g}_{\mathbb{C}}$ and $\mathfrak{j}$ is a real form of it with

$$\mathfrak{j} = \{A \in \mathfrak{j}_{\mathbb{C}} \mid \alpha(A) \in \mathbb{R} \text{ for any } \alpha \in \Delta\},$$

where Δ is the root system of $(\mathfrak{g}_{\mathbb{C}}, \mathfrak{j}_{\mathbb{C}})$. We put

$$\Sigma := \{\alpha|_{\mathfrak{a}} \mid \alpha \in \Delta\} \setminus \{0\} \subset \mathfrak{a}^*$$

to the restricted root system of $(\mathfrak{g}, \mathfrak{a})$. Then we can take a positive system Δ^+ of Δ such that the subset

$$\Sigma^+ := \{\alpha|_{\mathfrak{a}} \mid \alpha \in \Delta^+\} \setminus \{0\}.$$

of Σ becomes a positive system. In fact, if we take an ordering on $\mathfrak{a}$ and extend it to $\mathfrak{j}$, then the corresponding positive system Δ^+ satisfies the condition above. Let us denote by $W^{\mathbb{C}}$, W the Weyl groups of Δ, Σ, respectively. We set the closed positive Weyl chambers

$$\begin{aligned}\mathfrak{j}_+ &:= \{\, A \in \mathfrak{j} \mid \alpha(A) \geq 0 \quad \text{for any } \alpha \in \Delta^+ \,\},\\ \mathfrak{a}_+ &:= \{\, A \in \mathfrak{a} \mid \xi(A) \geq 0 \quad \text{for any } \xi \in \Sigma^+ \,\}.\end{aligned}$$

Then $\mathfrak{j}_+$ and $\mathfrak{a}_+$ are fundamental domains of $\mathfrak{j}$, $\mathfrak{a}$ for the actions of $W^{\mathbb{C}}$ and W, respectively. By the definition of Δ^+ and Σ^+, we have $\mathfrak{a}_+ = \mathfrak{j}_+ \cap \mathfrak{a}$.

Let w_0 denote the longest element of W with respect to the positive system Σ^+. Then the linear transform $x \mapsto -w_0 \cdot x$ on $\mathfrak{a}$ leaves the closed Weyl chamber $\mathfrak{a}_+$ invariant. As in Y. Benoist [3], we define a subspace $\mathfrak{b}$ in $\mathfrak{a}$ by

$$\mathfrak{b} := \mathfrak{a}^{-w_0} = \{\, A \in \mathfrak{a} \mid -w_0 \cdot A = A \,\}.$$

2.2. Satake diagram

We recall some facts for Satake diagrams of $\mathfrak{g}$ and weighted Dynkin diagrams corresponding to elements in $\mathfrak{a}_+$ in this subsection.

Let us denote by Π the fundamental system of Δ^+. Then

$$\overline{\Pi} := \{\, \alpha|_{\mathfrak{a}} \mid \alpha \in \Pi \,\} \setminus \{0\}$$

is the fundamental system of Σ^+. The Satake diagram $S_{\mathfrak{g}}$ of a semisimple Lie algebra $\mathfrak{g}$ consists of the following three data: the Dynkin diagram of $\mathfrak{g}_{\mathbb{C}}$ with nodes Π; black nodes $\Pi_0 := \{\alpha \in \Pi \mid \alpha|_{\mathfrak{a}} = 0\}$ in S; and arrows joining $\alpha \in \Pi \setminus \Pi_0$ and $\beta \in \Pi \setminus \Pi_0$ in S whose restrictions to $\mathfrak{a}$ are the same (see [1, 10] for more details).

For any $A \in \mathfrak{j}$, we can define a map

$$\Psi_A : \Pi \to \mathbb{R},\ \alpha \mapsto \alpha(A).$$

We call Ψ_A the weighted Dynkin diagram corresponding to $A \in \mathfrak{j}$, and $\alpha(A)$ the weight on a node $\alpha \in \Pi$ of the weighted Dynkin diagram. Since Π is a basis of $\mathfrak{j}^*$, the correspondence

$$\Psi : \mathfrak{j} \to \mathrm{Map}(\Pi, \mathbb{R}),\ A \mapsto \Psi_A \tag{2.1}$$

is a linear isomorphism between real vector spaces. In particular, Ψ is bijective, and hence

$$\Psi|_{\mathfrak{j}_+} : \mathfrak{j}_+ \to \mathrm{Map}(\Pi, \mathbb{R}_{\geq 0}),\ A \mapsto \Psi_A$$

is also bijective. We say that a weighted Dynkin diagram is trivial if all weights are zero. Namely, the trivial diagram corresponds to the zero in $\mathfrak{j}$ by Ψ.

Here, we recall the definition of weighted Dynkin diagrams *matching* the Satake diagram $S_{\mathfrak{g}}$ of $\mathfrak{g}$ as follows:

Definition 2.1 ([9, Definition 7.3]). Let $\Psi \in \mathrm{Map}(\Pi, \mathbb{R})$ be a weighted Dynkin diagram of $\mathfrak{g}_{\mathbb{C}}$ and $S_{\mathfrak{g}}$ the Satake diagram of $\mathfrak{g}$ with nodes Π. We say that Ψ *matches* $S_{\mathfrak{g}}$ if all the weights on black nodes in Π_0 are zero and any pair of nodes joined by an arrow have the same weights.

Then the following lemma holds:

Lemma 2.2 ([9, Lemma 7.5]). *The linear isomorphism* $\Psi : \mathfrak{j} \to \mathrm{Map}(\Pi, \mathbb{R})$ *induces a linear isomorphism*

$$\mathfrak{a} \to \{\, \Psi_A \in \mathrm{Map}(\Pi, \mathbb{R}) \mid \Psi_A \textit{ matches } S_{\mathfrak{g}} \,\},\quad A \mapsto \Psi_A.$$

In particular, by this linear isomorphism, we have

$$\mathfrak{a}_+ \overset{1:1}{\longleftrightarrow} \{\, \Psi_A \in \mathrm{Map}(\Pi, \mathbb{R}_{\geq 0}) \mid \Psi_A \textit{ matches } S_{\mathfrak{g}} \,\}.$$

2.3. Weighted Dynkin diagrams corresponding to elements in $\mathfrak{b}$

In this subsection, we recall an algorithm to classify all weighted Dynkin diagrams corresponding to elements in $\mathfrak{b} = \mathfrak{a}^{-w_0}$ (see (2.2)) by using the Satake diagram of $\mathfrak{g}$ and the opposition involution on the Dynkin diagram of $\mathfrak{g}_{\mathbb{C}}$ studied by Tits [11].

Let us denote by $w_0^{\mathbb{C}}$ the longest element of $W^{\mathbb{C}}$ corresponding to the positive system Δ^+. Then, by the action of $w_0^{\mathbb{C}}$, every element in $\mathfrak{j}_+$ moves to $-\mathfrak{j}_+ := \{-A \mid A \in \mathfrak{j}_+\}$. In particular,

$$-w_0^{\mathbb{C}} : \mathfrak{j} \to \mathfrak{j}, \quad A \mapsto -(w_0^{\mathbb{C}} \cdot A)$$

is an involutive automorphism on $\mathfrak{j}$ preserving $\mathfrak{j}_+$. We put

$$\mathfrak{j}^{-w_0^{\mathbb{C}}} := \{\, A \in \mathfrak{j} \mid -w_0^{\mathbb{C}} \cdot A = A \,\}.$$

Recall that the map $\Psi : \mathfrak{j} \to \mathrm{Map}(\Pi, \mathbb{R})$ in Section 2.2 is a linear isomorphism. Thus $-w_0^{\mathbb{C}}$ induces an involutive endomorphism on $\mathrm{Map}(\Pi, \mathbb{R})$, which will be denoted by ι. In other words, the involution ι on $\mathrm{Map}(\Pi, \mathbb{R})$ is induced by the opposition involution $\Pi \to \Pi, \alpha \mapsto -(w_0^{\mathbb{C}})^* \cdot \alpha$ (see Tits [11, Section 1.5.1] for more details).

Then we have

$$\Psi(\mathfrak{j}^{-w_0^{\mathbb{C}}}) = \mathrm{Map}(\Pi, \mathbb{R})^{\iota},$$

where $\mathrm{Map}(\Pi, \mathbb{R})^{\iota}$ denote the set of all weighted Dynkin diagrams held invariant by ι. For each complex simple Lie algebra $\mathfrak{g}_{\mathbb{C}}$, we determine ι as follows:

PROPOSITION 2.3 ([9, Theorem 6.3]). *Suppose that $\mathfrak{g}_{\mathbb{C}}$ is simple. The involution ι is not identity if and only if $\mathfrak{g}_{\mathbb{C}}$ is of type A_n, D_{2k+1} or E_6 $(n \geq 2,\ k \geq 2)$. In other words, this is the complete list of simple $\mathfrak{g}_{\mathbb{C}}$ with $\mathfrak{j}^{-w_0^{\mathbb{C}}} \neq \mathfrak{j}$. In such cases, the forms of ι are the following*:

For type A_n ($n \geq 2$, $\mathfrak{g}_{\mathbb{C}} \simeq \mathfrak{sl}(n+1,\mathbb{C})$)

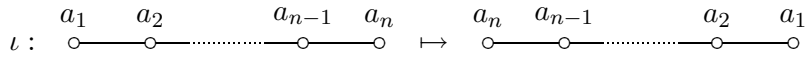

For type D_{2k+1} ($k \geq 2$, $\mathfrak{g}_{\mathbb{C}} \simeq \mathfrak{so}(4k+2,\mathbb{C})$)

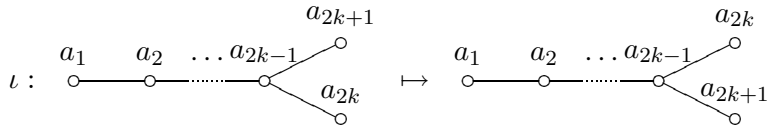

For type E_6 ($\mathfrak{g}_{\mathbb{C}} \simeq \mathfrak{e}_{6,\mathbb{C}}$)

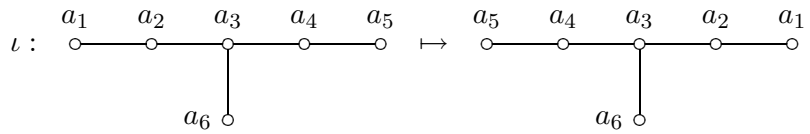

It should be noted that for the case where $\mathfrak{g}_{\mathbb{C}}$ is of type D_{2k} ($k \geq 2$), the involution $-w_0^{\mathbb{C}}$ on $\mathfrak{j}$ is trivial although the Dynkin diagram of type D_{2k} admits some non-trivial involutive automorphisms.

To classify elements in $\mathfrak{b}$, we use the following lemma:

Lemma 2.4 ([9, Lemma 7.6]). $\mathfrak{b} = \mathfrak{j}^{-w_0^{\mathbb{C}}} \cap \mathfrak{a}$.

By combining Lemma 2.2 with Lemma 2.4, we obtain that

$$\Psi(\mathfrak{b}) = \{\, \Psi_A \in \mathrm{Map}(\Pi,\mathbb{R})^{\iota} \mid \Psi_A \text{ matches } S_{\mathfrak{g}} \,\}. \tag{2.2}$$

where $\mathrm{Map}(\Pi,\mathbb{R})^{\iota}$ denote the set of all weighted Dynkin diagrams held invariant by ι, and S_g is the Satake diagram of $\mathfrak{g}$ (see Section 2.2).

2.4. The Dynkin–Kostant classification

In this subsection, we recall the Dynkin–Kostant classification of complex nilpotent orbits in a complex semisimple Lie algebra $\mathfrak{g}_{\mathbb{C}}$.

Let us denote by $\mathrm{Hom}(\mathfrak{sl}(2,\mathbb{C}),\mathfrak{g}_{\mathbb{C}})$ the set of all complex Lie algebra homomorphisms from $\mathfrak{sl}(2,\mathbb{C})$ to $\mathfrak{g}_{\mathbb{C}}$. For each $\rho \in \mathrm{Hom}(\mathfrak{sl}(2,\mathbb{C}),\mathfrak{g}_{\mathbb{C}})$, there uniquely exists an element A_ρ of $\mathfrak{j}_+$ which is conjugate to the element

$$\rho\begin{pmatrix}1 & 0\\ 0 & -1\end{pmatrix} \in \mathfrak{g}_{\mathbb{C}}$$

under the adjoint action on $\mathfrak{g}_{\mathbb{C}}$. Then the correspondence $[\rho] \mapsto A_\rho$ gives a map from $\mathrm{Hom}(\mathfrak{sl}(2,\mathbb{C}),\mathfrak{g}_{\mathbb{C}})/\mathrm{Int}\,\mathfrak{g}_{\mathbb{C}}$ to $\mathfrak{j}_+$. Malcev [8] proved that the map

$$\mathrm{Hom}(\mathfrak{sl}(2,\mathbb{C}),\mathfrak{g}_{\mathbb{C}})/\mathrm{Int}\,\mathfrak{g}_{\mathbb{C}} \hookrightarrow \mathfrak{j}_+,\ [\rho] \mapsto A_\rho$$

is injective. We put $\mathcal{H}^n(\mathfrak{j}_+)$ the image of the injective map above. Obviously, we have

$$\mathcal{H}^n(\mathfrak{j}_+) = \mathfrak{j}_+ \cap \left\{ \rho\begin{pmatrix}1 & 0\\ 0 & -1\end{pmatrix} \mid \rho \in \mathrm{Hom}(\mathfrak{sl}(2,\mathbb{C}),\mathfrak{g}_{\mathbb{C}}) \right\}.$$

Recall that Ψ in Section 2.2 induces a bijection between $\mathfrak{j}_+$ and $\mathrm{Map}(\Pi,\mathbb{R}_{\geq 0})$. Thus, a classification of $\Psi(\mathcal{H}^n(\mathfrak{j}_+))$ gives that of $\mathrm{Hom}(\mathfrak{sl}(2,\mathbb{C}),\mathfrak{g}_{\mathbb{C}})/\mathrm{Int}\,\mathfrak{g}_{\mathbb{C}}$. Dynkin [5] proved that any weight of an weighted Dynkin diagram in $\Psi(\mathcal{H}^n(\mathfrak{j}_+))$ is given by 0, 1 or 2. Hence, $\Psi(\mathcal{H}^n(\mathfrak{j}_+))$ (and therefore the set $\mathrm{Hom}(\mathfrak{sl}(2,\mathbb{C}),\mathfrak{g}_{\mathbb{C}})/\mathrm{Int}\,\mathfrak{g}_{\mathbb{C}}$ is) finite. Dynkin [5] also gave a complete list of the weighted Dynkin diagrams in $\Psi(\mathcal{H}^n(\mathfrak{j}_+))$ for each simple $\mathfrak{g}_{\mathbb{C}}$.

By combining the Jacobson–Morozov theorem with the results of Kostant [7], we also obtain a bijection

$$\mathrm{Hom}(\mathfrak{sl}(2,\mathbb{C}),\mathfrak{g}_{\mathbb{C}})/\mathrm{Int}\,\mathfrak{g}_{\mathbb{C}} \xrightarrow{\sim} \mathcal{N}(\mathfrak{g}_{\mathbb{C}})/\mathrm{Int}\,\mathfrak{g}_{\mathbb{C}},\ [\rho] \mapsto \mathrm{Int}\,\mathfrak{g}_{\mathbb{C}} \cdot \rho\begin{pmatrix}0 & 1\\ 0 & 0\end{pmatrix}.$$

Here $\mathcal{N}(\mathfrak{g}_{\mathbb{C}})/\mathrm{Int}\,\mathfrak{g}_{\mathbb{C}}$ denote the set of all complex nilpotent adjoint orbits in $\mathfrak{g}_{\mathbb{C}}$. Thus, the classification of $\Psi(\mathcal{H}^n(\mathfrak{j}_+))$, done by Dynkin [5], gives a classification of complex nilpotent adjoint orbits in $\mathfrak{g}_{\mathbb{C}}$ (see Bala–Cater [2] or Collingwood–McGovern [4, Section 3] for more details). This is known as the Dynkin–Kostant classification of complex nilpotent adjoint orbits.

2.5. Algorithm to classify hyperbolic elements coming from nilpotent orbits

In this subsection, we give an algorithm to determine the finite subset

$$\mathcal{H}^n(\mathfrak{a}_+) := \mathfrak{a}_+ \cap \left\{ \rho\begin{pmatrix}1 & 0\\ 0 & -1\end{pmatrix} \mid \rho \in \mathrm{Hom}(\mathfrak{sl}(2,\mathbb{R}),\mathfrak{g}) \right\}$$

of $\mathfrak{a}_+$ where $\mathrm{Hom}(\mathfrak{sl}(2,\mathbb{R}),\mathfrak{g})$ is the set of all Lie algebra homomorphisms from $\mathfrak{sl}(2,\mathbb{R})$ to $\mathfrak{g}$ as in Section 1. We note that similar to the situation for $\mathfrak{g}_{\mathbb{C}}$, for any $\rho \in \mathrm{Hom}(\mathfrak{sl}(2,\mathbb{R}),\mathfrak{g})$, there uniquely exists $A_\rho \in \mathcal{H}^n(\mathfrak{a}_+)$ such that $\rho\begin{pmatrix}1 & 0\\ 0 & -1\end{pmatrix}$ is conjugate to A_ρ under the adjoint action on $\mathfrak{g}$.

Recall that $\mathfrak{g} = \mathfrak{k} + \mathfrak{p}$ is a real form of $\mathfrak{g}_{\mathbb{C}}$, $\mathfrak{j} = \sqrt{-1}\mathfrak{t} + \mathfrak{a}$ and $\mathfrak{a}_+ = \mathfrak{a} \cap \mathfrak{j}_+$ in our setting. Then by [9, Proposition 4.5 (iii)], we have $\mathcal{H}^n(\mathfrak{a}_+) = \mathfrak{a}_+ \cap \mathcal{H}^n(\mathfrak{j}_+)$. Therefore, by Lemma 2.2, the following holds

$$\Psi(\mathcal{H}^n(\mathfrak{a}_+)) = \{\Psi_A \in \Psi(\mathcal{H}^n(\mathfrak{j}_+)) \mid \Psi_A \text{ matches } S_{\mathfrak{g}}\}, \tag{2.3}$$

where $S_{\mathfrak{g}}$ is the Satake diagram of $\mathfrak{g}$ (see Section 2.2 for the notation). Hence, for each $\mathfrak{g}$, by using the classification of $\Psi(\mathcal{H}^n(\mathfrak{j}_+))$ (see Section 2.4) and the Satake diagram $S_{\mathfrak{g}}$ of $\mathfrak{g}$, we obtain a classification of $\Psi(\mathcal{H}^n(\mathfrak{a}_+))$.

REMARK 2.5. The finite set $\mathcal{H}^n(\mathfrak{a}_+)$ parametrizes the set $\mathcal{N}_{\mathfrak{g}}(\mathfrak{g}_{\mathbb{C}})/\mathrm{Int}\,\mathfrak{g}_{\mathbb{C}}$ of complex nilpotent adjoint orbits in $\mathfrak{g}_{\mathbb{C}}$ that meet the real form $\mathfrak{g}$, i.e. there is a natural bijection

$$\varphi : \mathcal{H}^n(\mathfrak{a}_+) \xrightarrow{\sim} \mathcal{N}_{\mathfrak{g}}(\mathfrak{g}_{\mathbb{C}})/\mathrm{Int}\,\mathfrak{g}_{\mathbb{C}}, \quad \rho\begin{pmatrix}1 & 0\\ 0 & -1\end{pmatrix} \mapsto (\mathrm{Int}\,\mathfrak{g}_{\mathbb{C}})\cdot\rho\begin{pmatrix}0 & 1\\ 0 & 0\end{pmatrix}$$

(see [9, Section 7.4] for more details). We note that $\mathcal{H}^n(\mathfrak{a}_+)$ is not bijective to the set $\mathcal{N}(\mathfrak{g})/\mathrm{Int}\,\mathfrak{g}$ of real nilpotent adjoint orbits in $\mathfrak{g}$. In fact, the surjective map $\phi : \mathcal{N}(\mathfrak{g})/\mathrm{Int}\,\mathfrak{g} \twoheadrightarrow \mathcal{H}^n(\mathfrak{a}_+)$ defined in Section 1 is not always injective. In summary, we have the following commutative diagram:

$$\begin{array}{ccc} \mathcal{N}_{\mathfrak{g}}(\mathfrak{g}_{\mathbb{C}})/\mathrm{Int}\,\mathfrak{g}_{\mathbb{C}} & \xleftarrow[\varphi]{\sim} & \mathcal{H}^n(\mathfrak{a}_+) \\ \text{complexification}\uparrow & \nearrow_{\phi} & \\ \mathcal{N}(\mathfrak{g})/\mathrm{Int}\,\mathfrak{g} & & \end{array}$$

where the complexification of a real nilpotent adjoint orbit $\mathcal{O}$ in $\mathfrak{g}$ is defined as $(\mathrm{Int}\,\mathfrak{g}_{\mathbb{C}})\cdot\mathcal{O} \subset \mathfrak{g}_{\mathbb{C}}$. The survey of classifications of real nilpotent (adjoint) orbits in semisimple Lie algebras can be found in [4, Chapter 9].

3. Proof of Theorem 1.1

First, we show the easy part of Theorem 1.1 as follows:

LEMMA 3.1. $\mathcal{H}^n(\mathfrak{a}_+) \subset \mathfrak{b}$ $(:= \mathfrak{a}^{-w_0})$.

PROOF OF LEMMA 3.1. Let us fix any $\rho \in \mathrm{Hom}(\mathfrak{sl}(2,\mathbb{R}), \mathfrak{g})$ with $A_\rho := \rho\begin{pmatrix} 1 & 0 \\ 0 & -1 \end{pmatrix} \in \mathfrak{a}_+$. It is enough to show that $-A_\rho = w_0 A_\rho$. We denote by $\tilde{\rho} : PSL(2,\mathbb{R}) \to \mathrm{Int}\,\mathfrak{g}$ the Lie group homomorphism corresponding to $\rho : \mathfrak{sl}(2,\mathbb{R}) \to \mathfrak{g}$.

One can observe that, in $\mathfrak{sl}(2,\mathbb{R})$, the two elements $\begin{pmatrix} 1 & 0 \\ 0 & -1 \end{pmatrix}$ and $\begin{pmatrix} -1 & 0 \\ 0 & 1 \end{pmatrix}$ are conjugate under the adjoint action of $PSL(2,\mathbb{R})$. Therefore two elements $A_\rho, -A_\rho \in \mathfrak{g}$ are conjugate under the adjoint action of $\tilde{\rho}(PSL(2,\mathbb{R})) \subset \mathrm{Int}\,\mathfrak{g}$. On the other hand, for any $A \in \mathfrak{a}_+ \subset \mathfrak{g}$, we have that

$$(\mathrm{Int}\,\mathfrak{g} \cdot A) \cap \mathfrak{a} = W \cdot A$$

(see [9, Lemma 7.2] for more details). Hence for $A_\rho \in \mathfrak{a}_+$, the element $-A_\rho$ is in $W \cdot A_\rho$. Since $-A_\rho \in -\mathfrak{a}_+$, we have $-A_\rho = w_0 A_\rho$. □

In the rest of this section, we give a proof of non-trivial part $\mathfrak{b} \subset \mathbb{R}\text{-span}(\mathcal{H}^n(\mathfrak{a}_+))$ of Theorem 1.1.

Recall that $\Psi : \mathfrak{j} \to \mathrm{Map}(\Pi, \mathbb{R})$ in Section 2.2 is a linear isomorphism. Therefore, to complete the proof of Theorem 1.1, we only need to show that

$$\Psi(\mathfrak{b}) \subset \mathbb{R}\text{-span}\Psi(\mathcal{H}^n(\mathfrak{a}_+)) \tag{3.1}$$

We note that our claim for semisimple $\mathfrak{g}$ is reduced to that on each simple factor of $\mathfrak{g}$. Furthermore, in the case where $\mathfrak{g}$ is a complex simple Lie algebra, our claim is reduced to the case where $\mathfrak{g}'$ is a split real form of $\mathfrak{g}$. Thus, it is enough to show (3.1) for the case where $\mathfrak{g}_{\mathbb{C}}$ is simple and $\mathfrak{g}$ is non-compact real form of $\mathfrak{g}_{\mathbb{C}}$. To do this, we shall find weighted Dynkin diagrams $\Psi_1, \ldots, \Psi_n$ in $\Psi(\mathcal{H}^n(\mathfrak{a}_+))$ such that $\{\Psi_1, \ldots, \Psi_n\}$ becomes a basis of $\Psi(\mathfrak{b})$ for each non-compact real simple Lie algebra $\mathfrak{g}$.

In the rest of this section, for each complex simple $\mathfrak{g}_{\mathbb{C}}$, we give an explicit form of $\mathrm{Map}(\Pi, \mathbb{R})^\iota$ (see Section 2.3 for the definition of ι) and some examples in $\Psi(\mathcal{H}^n(\mathfrak{j}_+))$ from the list given by Dynkin [5] (we will refer [4] for classifications of weighted Dynkin diagrams in $\Psi(\mathcal{H}^n(\mathfrak{j}_+))$). Then for

each non-compact real form $\mathfrak{g}$ of $\mathfrak{g}_{\mathbb{C}}$, we give the Satake diagram $S_{\mathfrak{g}}$ of $\mathfrak{g}$, which can be found in [1], and the explicit form of $\Psi(\mathfrak{b})$ by using (2.2) in Section 2.3. Finally, for each $\mathfrak{g}$, we give an example of a basis $\{\Psi_1, \dots, \Psi_n\}$ of $\Psi(\mathfrak{b})$ with

$$\Psi_i \in \Psi(\mathcal{H}^n(\mathfrak{a}_+)) = \{\Psi_A \in \Psi(\mathcal{H}^n(\mathfrak{j}_+)) \mid \Psi_A \text{ matches } S_{\mathfrak{g}}\}$$

(see Section 2.5 for the details). Then the proof of Theorem 1.1 will be completed.

REMARK 3.2. As in the following subsections, our basis $\{\Psi_1, \dots, \Psi_n\}$ of $\Psi(\mathfrak{b})$ consists of weighted Dynkin diagrams of even nilpotent orbits, where "even" means that any weight of Ψ_i is 0 or 2.

3.1. Type A_l

Let us consider the case where $\mathfrak{g}_{\mathbb{C}}$ is of type A_l for $l \geq 1$, that is, $\mathfrak{g}_{\mathbb{C}} \simeq \mathfrak{sl}(l+1, \mathbb{C})$. Then we have

$$\mathrm{Map}(\Pi, \mathbb{R})^{\iota} = \left\{ \begin{array}{ccccccc} a_1 & a_2 & \dots & a_{l-1} & a_l \\ \circ\!\!-\!\!\!-\!\!\circ & -\!\!\circ\!\!-\!\!\!-\!\!\circ & \cdots & \circ\!\!-\!\!\!-\!\!\circ & -\!\!\circ \end{array} \;\middle|\; a_i = a_{l+1-i} \text{ for } i = 1, \dots, l \right\}$$

By [4, Section 3.6], we can find some examples of weighted Dynkin diagrams in $\Psi(\mathcal{H}^n(\mathfrak{j}_+))$ as in Table 3.1.1 below.

Table 3.1.1. Examples of weighted Dynkin diagrams in $\Psi(\mathcal{H}^n(\mathfrak{j}_+))$ of type A_l.

Symbol	Weighted Dynkin diagram in $\Psi(\mathcal{H}^n(\mathfrak{j}_+))$
$[l+1]$	$\overset{2}{\circ}\!\!-\!\!\overset{2}{\circ}\!\!-\cdots-\!\!\overset{2}{\circ}\!\!-\!\!\overset{2}{\circ}$
$[2s+1, 1^{l-2s}]$	$\overset{2}{\circ}\cdots\overset{2}{\circ}\!\!-\!\!\overset{2}{\circ}\!\!-\!\!\overset{0}{\circ}\cdots\overset{0}{\circ}\!\!-\!\!\overset{2}{\circ}\!\!-\!\!\overset{2}{\circ}\cdots\overset{2}{\circ}$ $\alpha_s \qquad\qquad \alpha_{l+1-s}$
$[(2s+1)^2, 1^{l-4s-1}]$	$\overset{0}{\circ}\!\!-\!\!\overset{2}{\circ}\!\!-\!\!\overset{0}{\circ}\!\!-\!\!\overset{2}{\circ}\cdots\overset{0}{\circ}\!\!-\!\!\overset{2}{\circ}\!\!-\!\!\overset{0}{\circ}\!\!-\!\!\overset{0}{\circ}\cdots\overset{0}{\circ}\!\!-\!\!\overset{0}{\circ}\!\!-\!\!\overset{2}{\circ}\!\!-\!\!\overset{0}{\circ}\cdots\overset{2}{\circ}\!\!-\!\!\overset{0}{\circ}\!\!-\!\!\overset{2}{\circ}\!\!-\!\!\overset{0}{\circ}$ $\alpha_{2s} \qquad\qquad \alpha_{l+1-2s}$

The Satake diagrams $S_{\mathfrak{g}}$ and $\Psi(\mathfrak{b})$ of non-compact real forms $\mathfrak{g}$ of $\mathfrak{g}_{\mathbb{C}}$ are listed in Table 3.1.2 below.

Therefore for each $\mathfrak{g}$, we can find a basis of $\Psi(\mathfrak{b})$ by taking some weighted Dynkin diagrams in $\Psi(\mathcal{H}^n(\mathfrak{a}_+)) = \{\Psi_A \in \Psi(\mathcal{H}^n(\mathfrak{j}_+)) \mid \Psi_A \text{ matches } S_{\mathfrak{g}}\}$ as in Table 3.1.3 below.

Table 3.1.2. List of Satake diagrams and $\Psi(\mathfrak{b})$ of type A_l.

$\mathfrak{g}$	$S_{\mathfrak{g}}$	$\Psi(\mathfrak{b})$
$\mathfrak{sl}(l+1,\mathbb{R})$	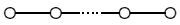	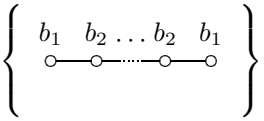
$\mathfrak{su}^*(2k)$ $(2k = l+1)$	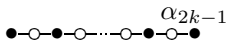	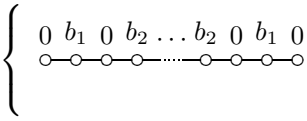
$\mathfrak{su}(p,q)$ $(p+q = l+1)$ $(p > q+1)$	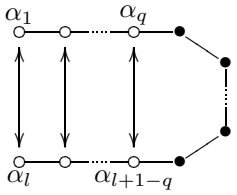	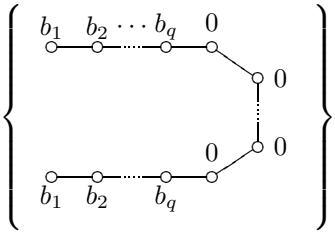
$\mathfrak{su}(k+1,k)$ $(2k = l)$	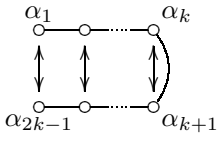	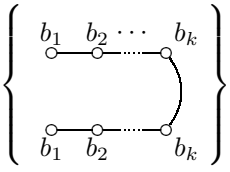
$\mathfrak{su}(k,k)$ $(2k = l+1)$	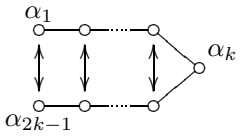	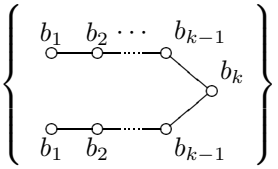

Table 3.1.3. Examples of bases of $\Psi(\mathfrak{b})$ for real forms of type A_l.

$\mathfrak{g}$	Example of a basis of $\Psi(\mathfrak{b})$
$\mathfrak{sl}(2k,\mathbb{R})$ $(2k=l+1)$	$[3,1^{2k-3}],[5,1^{2k-5}],\dots,[2k-1,1],[2k]$
$\mathfrak{sl}(2k+1,\mathbb{R})$ $(2k=l)$	$[3,1^{2k-2}],[5,1^{2k-4}],\dots,[2k+1]$
$\mathfrak{su}^*(4m)$ $(4m=l+1)$	$[3^2,1^{4m-6}],[5^2,1^{4m-10}],\dots,$ $[(2m-1)^2,1^2],[(2m)^2]$
$\mathfrak{su}^*(4m+2)$ $(4m=l-1)$	$[3^2,1^{4m-4}],[5^2,1^{4m-8}],\dots,[(2m+1)^2]$
$\mathfrak{su}(p,q)$ $(p+q=l+1,p>q+1)$	$[3,1^{l-2}],[5,1^{l-4}],\dots,[2q+1,1^{l-2q}]$
$\mathfrak{su}(k+1,k)$ $(2k=l)$	$[3,1^{2k-2}],[5,1^{2k-4}],\dots,[2k-1,1^2],[2k+1]$
$\mathfrak{su}(k,k)$ $(2k=l+1)$	$[3,1^{2k-3}],[5,1^{2k-5}],\dots,[2k-1,1],[2k]$

3.2. Type B_l

Let us consider the case where $\mathfrak{g}_{\mathbb{C}}$ is of type B_l for $l \geq 1$, that is, $\mathfrak{g}_{\mathbb{C}} \simeq \mathfrak{so}(2l+1,\mathbb{C})$. Then we have

$$\mathrm{Map}(\Pi,\mathbb{R})^{\iota} = \mathrm{Map}(\Pi,\mathbb{R}) = \left\{ \begin{array}{c} \overset{a_1}{\circ}\!\!-\!\!\!-\overset{a_2}{\circ}\!\!-\!\!\cdots\!\!-\overset{a_{l-1}}{\circ}\!\!\Longrightarrow\!\!\overset{a_l}{\circ} \\ \\ \end{array} \right\}$$

By [4, Section 5.3], we can find some examples of weighted Dynkin diagrams in $\Psi(\mathcal{H}^n(\mathfrak{j}_+))$ as in Table 3.2.1 below.

Table 3.2.1. Examples of weighted Dynkin diagrams in $\Psi(\mathcal{H}^n(\mathfrak{j}_+))$ of type B_l.

Symbol	Weighted Dynkin diagram in $\Psi(\mathcal{H}^n(\mathfrak{j}_+))$
$[2l+1]$	$\overset{2}{\circ}\!\!-\!\!\overset{2}{\circ}\!\!-\!\!\cdots\!\!-\overset{2}{\circ}\!\!\Longrightarrow\!\!\overset{2}{\circ}$
$[2s+1,1^{2l-2s}]$	$\overset{2}{\circ}\!\!-\!\!\overset{2}{\circ}\!\!-\!\!\cdots\!\!-\overset{2}{\underset{\alpha_s}{\circ}}\!\!-\!\!\overset{0}{\circ}\!\!-\!\!\cdots\!\!-\overset{0}{\circ}\!\!\Longrightarrow\!\!\overset{0}{\circ}$

The Satake diagrams $S_{\mathfrak{g}}$ and $\Psi(\mathfrak{b})$ of non-compact real forms $\mathfrak{g}$ of $\mathfrak{g}_{\mathbb{C}}$ are listed in Table 3.2.2 below.

Therefore for each $\mathfrak{g}$, we can find a basis of $\Psi(\mathfrak{b})$ by taking some weighted Dynkin diagrams in $\Psi(\mathcal{H}^n(\mathfrak{a}_+)) = \{\Psi_A \in \Psi(\mathcal{H}^n(\mathfrak{j}_+)) \mid \Psi_A \text{ matches } S_{\mathfrak{g}}\}$ in Table 3.2.3 below.

Table 3.2.2. List of Satake diagrams and $\Psi(\mathfrak{b})$ of type B_l.

$\mathfrak{g}$	$S_{\mathfrak{g}}$	$\Psi(\mathfrak{b})$
$\mathfrak{so}(p,q)$ $(p+q=2l+1)$ $(p>q+1)$	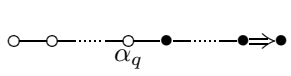	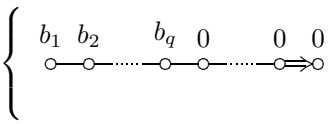
$\mathfrak{so}(l+1,l)$	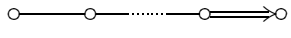	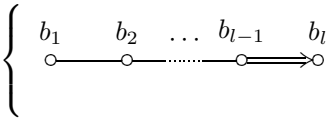

Table 3.2.3. Examples of bases of $\Psi(\mathfrak{b})$ for real forms of type B_l.

$\mathfrak{g}$	Example of a basis of $\Psi(\mathfrak{b})$
$\mathfrak{so}(p,q)$ $(p+q=2l+1, p>q+1)$	$[3,1^{2l-2}],[5,1^{2l-4}],\ldots,[2q+1,1^{2l-2q}]$
$\mathfrak{so}(l+1,l)$	$[3,1^{2l-2}],[5,1^{2l-4}],\ldots,[2l+1]$

3.3. Type C_l

Let us consider the case where $\mathfrak{g}_{\mathbb{C}}$ is of type C_l for $l \geq 1$, that is, $\mathfrak{g}_{\mathbb{C}} \simeq \mathfrak{sp}(l,\mathbb{C})$. Then we have

$$\mathrm{Map}(\Pi,\mathbb{R})^{\iota} = \mathrm{Map}(\Pi,\mathbb{R}) = \left\{ \begin{array}{c} \text{  } \end{array} \right\}$$

By [4, Section 5.3], we can find some examples of weighted Dynkin diagrams in $\Psi(\mathcal{H}^n(\mathfrak{j}_+))$ as in Table 3.3.1 below.

The Satake diagrams $S_{\mathfrak{g}}$ and $\Psi(\mathfrak{b})$ of non-compact real forms $\mathfrak{g}$ of $\mathfrak{g}_{\mathbb{C}}$ are listed in Table 3.3.2 below.

Table 3.3.1. Examples of weighted Dynkin diagrams in $\Psi(\mathcal{H}^n(\mathfrak{j}_+))$ of type C_l.

Symbol	Weighted Dynkin diagram in $\Psi(\mathcal{H}^n(\mathfrak{j}_+))$
$[2^l]$	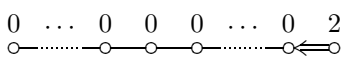
$[2s+2, 2^{l-s}]$	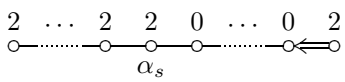
$[(2s+1)^2, 1^{2l-4s-2}]$	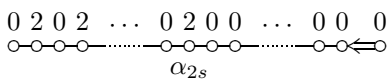
$[(2k)^2]$ $(2k=l)$	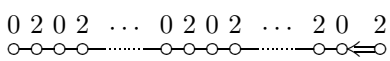

Table 3.3.2. List of Satake diagrams and $\Psi(\mathfrak{b})$ of type C_l.

$\mathfrak{g}$	$S_{\mathfrak{g}}$	$\Psi(\mathfrak{b})$
$\mathfrak{sp}(l,\mathbb{R})$	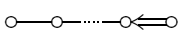	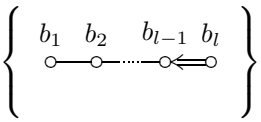
$\mathfrak{sp}(p,q)$ $(p+q=l)$ $(p>q)$	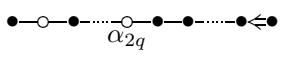	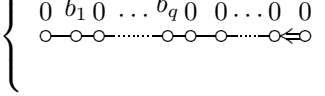
$\mathfrak{sp}(k,k)$ $(2k=l)$	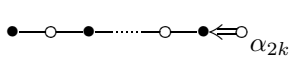	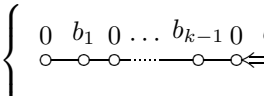

Therefore for each $\mathfrak{g}$, we can find a basis of $\Psi(\mathfrak{b})$ by taking some weighted Dynkin diagrams in $\Psi(\mathcal{H}^n(\mathfrak{a}_+)) = \{\Psi_A \in \Psi(\mathcal{H}^n(\mathfrak{j}_+)) \mid \Psi_A \text{ matches } S_{\mathfrak{g}}\}$ in Table 3.3.3 below.

Table 3.3.3. Examples of bases of $\Psi(\mathfrak{b})$ for real forms of type C_l.

$\mathfrak{g}$	Example of a basis of $\Psi(\mathfrak{b})$
$\mathfrak{sp}(l,\mathbb{R})$	$[2^l], [4, 2^{l-2}], [6, 2^{l-3}], \ldots, [2l]$
$\mathfrak{sp}(p,q)$ $(p+q=l, p>q)$	$[3^2, 1^{2l-6}], [5^2, 1^{2l-10}], \ldots, [(2q+1)^2, 1^{2l-2q-1}]$
$\mathfrak{sp}(k,k)$ $(2k=l)$	$[3^2, 1^{4k-6}], [5^2, 1^{4k-10}], \ldots, [(2k-1)^2, 1^2], [(2k)^2]$

3.4. Type D_{2m}

Let us consider the case where $\mathfrak{g}_{\mathbb{C}}$ is of type D_{2m} for $m \geq 2$, that is, $\mathfrak{g}_{\mathbb{C}} \simeq \mathfrak{so}(4m, \mathbb{C})$. Then we have

$$\mathrm{Map}(\Pi,\mathbb{R})^{\iota} = \mathrm{Map}(\Pi,\mathbb{R}) = \left\{ \right.$$

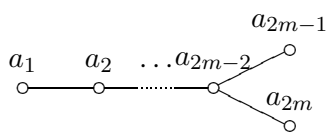

$$\left. \right\}$$

By [4, Section 5.3], we can find some examples of weighted Dynkin diagrams in $\Psi(\mathcal{H}^n(\mathfrak{j}_+))$ as in Table 3.4.1 below.

Table 3.4.1. Examples of weighted Dynkin diagrams in $\Psi(\mathcal{H}^n(\mathfrak{j}_+))$ of type D_{2m}.

Symbol	Weighted Dynkin diagram in $\Psi(\mathcal{H}^n(\mathfrak{j}_+))$
$[2s+1, 1^{4m-2s-1}]$	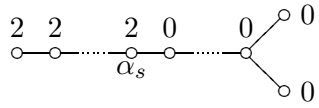

$[4m-1,1]$	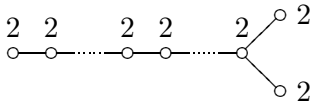
$[2^{2m}]_{\mathrm{I}}$	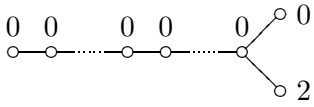
$[(2s+1)^2,1^{4m-4s-2}]$	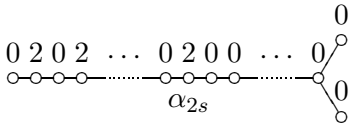

The Satake diagrams $S_{\mathfrak{g}}$ and $\Psi(\mathfrak{b})$ of non-compact real forms $\mathfrak{g}$ of $\mathfrak{g}_{\mathbb{C}}$ are listed in Table 3.4.2 below.

Table 3.4.2. List of Satake diagrams and $\Psi(\mathfrak{b})$ of type D_{2m}.

$\mathfrak{g}$	$S_{\mathfrak{g}}$	$\Psi(\mathfrak{b})$
$\mathfrak{so}(p,q)$ $(p+q=4m)$ $(p>q+2)$	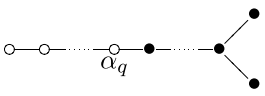	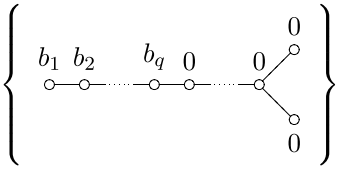
$\mathfrak{so}(2m+1,2m-1)$	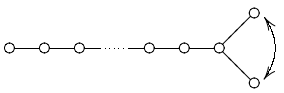	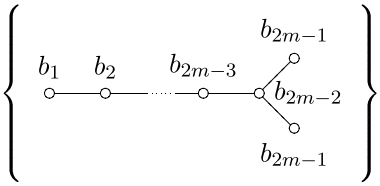
$\mathfrak{so}(2m,2m)$	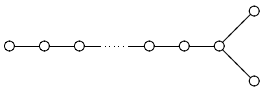	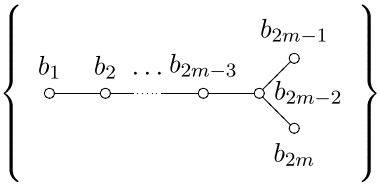

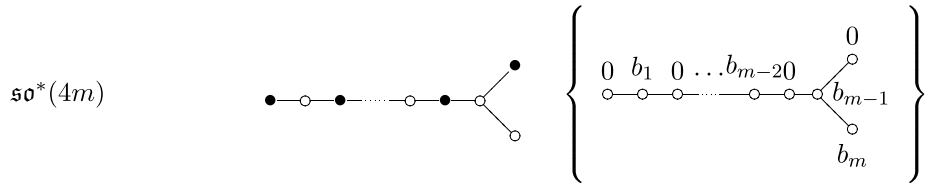

Therefore for each $\mathfrak{g}$, we can find a basis of $\Psi(\mathfrak{b})$ by taking some weighted Dynkin diagrams in $\Psi(\mathcal{H}^n(\mathfrak{a}_+)) = \{\Psi_A \in \Psi(\mathcal{H}^n(\mathfrak{j}_+)) \mid \Psi_A \text{ matches } S_\mathfrak{g}\}$ in Table 3.4.3 below.

Table 3.4.3. Examples of bases of $\Psi(\mathfrak{b})$ for real forms of type D_{2m}.

$\mathfrak{g}$	Example of a basis of $\Psi(\mathfrak{b})$
$\mathfrak{so}(p,q)$ $(p+q=4m, p>q+2)$	$[3,1^{4m-3}], [5,1^{4m-5}], \ldots, [2q+1,1^{4m-2q-1}]$
$\mathfrak{so}(2m+1,2m-1)$	$[3,1^{4m-3}], [5,1^{4m-5}], \ldots, [4m-1,1]$
$\mathfrak{so}(2m,2m)$	$[3,1^{4m-1}], [5,1^{4m-3}], \ldots, [4m-1,1], [2^{2m}]_{\mathrm{I}}$
$\mathfrak{so}^*(4m)$	$[3^2,1^{4m-6}], [5^2,1^{4m-10}], \ldots,$ $[(2m-1)^2,1^2], [2^{2m}]_{\mathrm{I}}$

3.5. Type D_{2m+1}

Let us consider the case where $\mathfrak{g}_\mathbb{C}$ is of type D_{2m+1} for $m \geq 1$, that is, $\mathfrak{g}_\mathbb{C} \simeq \mathfrak{so}(4m+2,\mathbb{C})$. Then we have

$$\mathrm{Map}(\Pi,\mathbb{R})^\iota = \left\{ \begin{array}{c|c} \begin{array}{l} \\ \\ \end{array} & a_{2m} = a_{2m+1} \end{array} \right\}$$

By [4, Section 5.3], we can find some examples of weighted Dynkin diagrams in $\Psi(\mathcal{H}^n(\mathfrak{j}_+))$ as in Table 3.5.1 below.

The Satake diagrams $S_\mathfrak{g}$ and $\Psi(\mathfrak{b})$ of non-compact real forms $\mathfrak{g}$ of $\mathfrak{g}_\mathbb{C}$ are listed in Table 3.5.2 below.

Table 3.5.1. Examples of weighted Dynkin diagrams in $\Psi(\mathcal{H}^n(\mathrm{j}_+))$ of type D_{2m+1}.

Symbol	Weighted Dynkin diagram in $\Psi(\mathcal{H}^n(\mathrm{j}_+))$
$[2s+1, 1^{4m-2s+1}]$	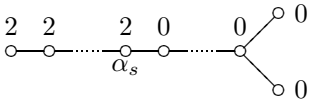
$[4m+1, 1]$	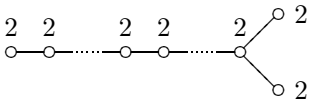
$[(2s+1)^2, 1^{4m-4s}]$	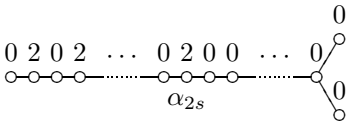
$[(2m+1)^2]$	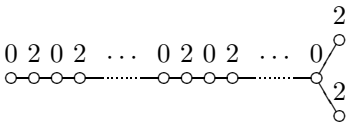

Table 3.5.2. List of Satake diagrams and $\Psi(\mathfrak{b})$ of type D_{2m+1}.

$\mathfrak{g}$	$S_{\mathfrak{g}}$	$\Psi(\mathfrak{b})$
$\mathfrak{so}(p,q)$ $(p+q=4m+2)$ $(p>q+2)$	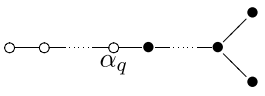	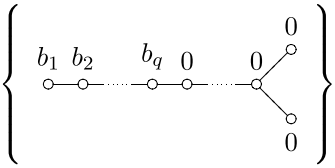
$\mathfrak{so}(2m+2, 2m)$	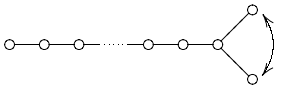	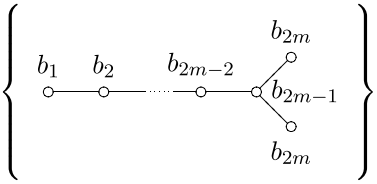

$\mathfrak{so}(2m+1, 2m+1)$	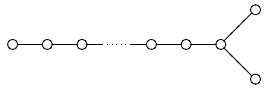	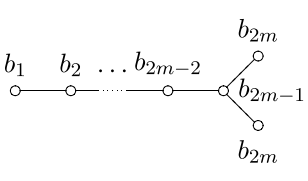
$\mathfrak{so}^*(4m+2)$	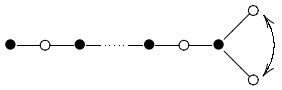	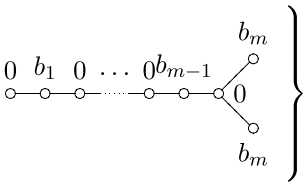

Therefore for each $\mathfrak{g}$, we can find a basis of $\Psi(\mathfrak{b})$ by taking some weighted Dynkin diagrams in $\Psi(\mathcal{H}^n(\mathfrak{a}_+)) = \{\Psi_A \in \Psi(\mathcal{H}^n(\mathfrak{j}_+)) \mid \Psi_A \text{ matches } S_{\mathfrak{g}}\}$ in Table 3.5.3 below.

Table 3.5.3. Examples of bases of $\Psi(\mathfrak{b})$ for real forms of type D_{2m+1}.

$\mathfrak{g}$	Example of a basis of $\Psi(\mathfrak{b})$
$\mathfrak{so}(p,q)$ $(p+q=4m+2, p>q+2)$	$[3,1^{4m-1}], [5,1^{4m-3}], \ldots, [2q+1,1^{4m-2q+1}]$
$\mathfrak{so}(2m+2,2m)$	$[3,1^{4m-1}], [5,1^{4m-3}], \ldots, [4m+1,1]$
$\mathfrak{so}(2m+1,2m+1)$	$[3,1^{4m-1}], [5,1^{4m-3}], \ldots, [4m+1,1]$
$\mathfrak{so}^*(4m+2)$	$[3^2,1^{4m-4}], [5^2,1^{4m-8}], \ldots, [(2m+1)^2]$

3.6. Type E_6

Let us consider the case where $\mathfrak{g}_{\mathbb{C}}$ is of type E_6, that is, $\mathfrak{g}_{\mathbb{C}} \simeq \mathfrak{e}_{6,\mathbb{C}}$. Then we have

$$\mathrm{Map}(\Pi, \mathbb{R})^{\iota} = \left\{ \begin{array}{c|c} \begin{array}{ccccc} a_1 & a_2 & a_3 & a_4 & a_5 \\ \circ & \circ & \circ & \circ & \circ \\ & & \circ & & \\ & & a_6 & & \end{array} & a_1 = a_5,\ a_2 = a_4 \end{array} \right\}$$

In [4, Section 8.4], we can find some examples of weighted Dynkin diagrams in $\Psi(\mathcal{H}^n(\mathfrak{j}_+))$ as in Table 3.6.1 below.

The Satake diagrams $S_{\mathfrak{g}}$ and $\Psi(\mathfrak{b})$ of non-compact real forms $\mathfrak{g}$ of $\mathfrak{g}_{\mathbb{C}}$ are listed in Table 3.6.2 below.

Table 3.6.1. Examples of weighted Dynkin diagrams in $\Psi(\mathcal{H}^n(\mathfrak{j}_+))$ of type E_6.

Symbol	Weighted Dynkin diagram in $\Psi(\mathcal{H}^n(\mathfrak{j}_+))$
A_2	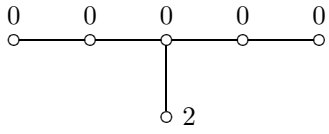
$2A_2$	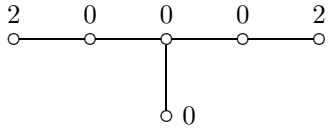
D_4	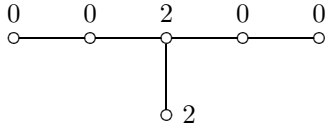
E_6	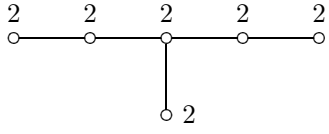

Table 3.6.2. List of Satake diagrams and $\Psi(\mathfrak{b})$ of type E_6.

$\mathfrak{g}$	$S_{\mathfrak{g}}$	$\Psi(\mathfrak{b})$
$\mathfrak{e}_{6(6)}$	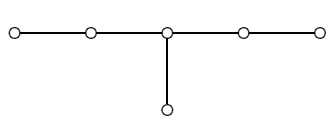	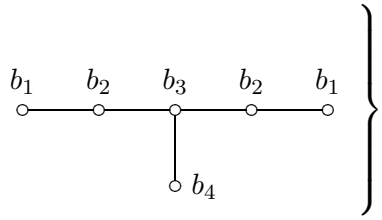

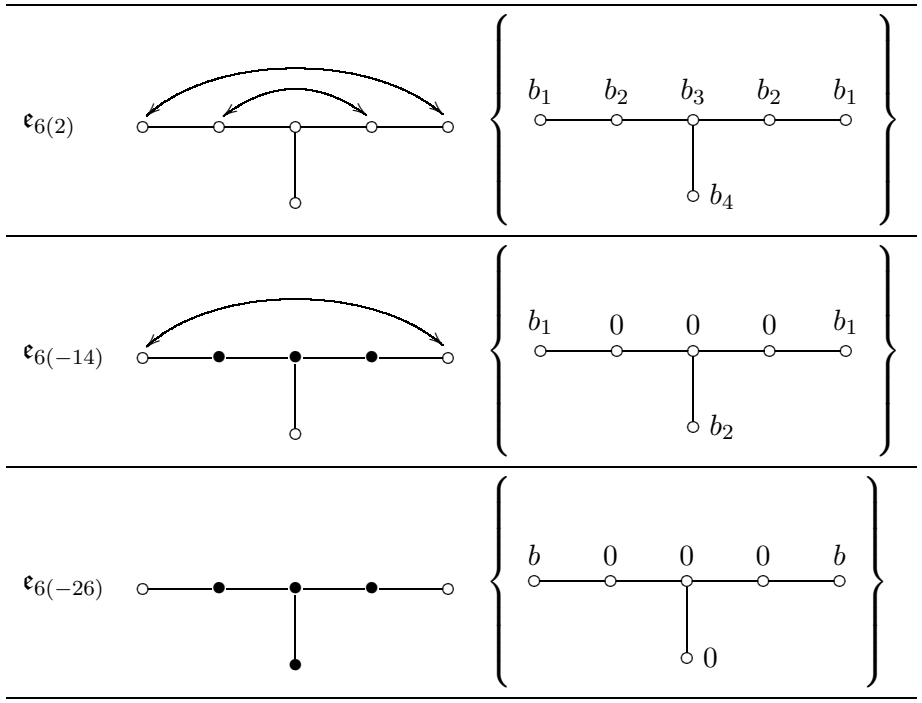

Therefore for each $\mathfrak{g}$, we can find a basis of $\Psi(\mathfrak{b})$ by taking some weighted Dynkin diagrams in $\Psi(\mathcal{H}^n(\mathfrak{a}_+)) = \{\Psi_A \in \Psi(\mathcal{H}^n(\mathfrak{j}_+)) \mid \Psi_A \text{ matches } S_{\mathfrak{g}}\}$ in Table 3.6.3 below.

Table 3.6.3. Examples of bases of $\Psi(\mathfrak{b})$ for real forms of type E_6.

$\mathfrak{g}$	Example of a basis of $\Psi(\mathfrak{b})$
$\mathfrak{e}_{6(6)}$	$A_2, 2A_2, D_4, E_6$
$\mathfrak{e}_{6(2)}$	$A_2, 2A_2, D_4, E_6$
$\mathfrak{e}_{6(-14)}$	$A_2, 2A_2$
$\mathfrak{e}_{6(-26)}$	$2A_2$

3.7. Type E_7

Let us consider the case where $\mathfrak{g}_{\mathbb{C}}$ is of type E_7, that is, $\mathfrak{g}_{\mathbb{C}} \simeq \mathfrak{e}_{7,\mathbb{C}}$. Then we have

$$\mathrm{Map}(\Pi, \mathbb{R})^{\iota} = \mathrm{Map}(\Pi, \mathbb{R}) = \left\{ \right.$$

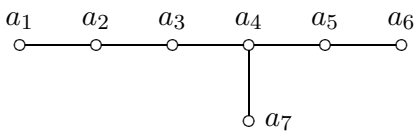

$$\left. \right\}$$

In [4, Section 8.4], we can find some examples of weighted Dynkin diagrams in $\Psi(\mathcal{H}^n(\mathrm{j}_+))$ as in Table 3.7.1 below.

Table 3.7.1. Examples of weighted Dynkin diagrams in $\Psi(\mathcal{H}^n(\mathrm{j}_+))$ of type E_7.

Symbol	Weighted Dynkin diagram in $\Psi(\mathcal{H}^n(\mathrm{j}_+))$
$(3A_1)''$	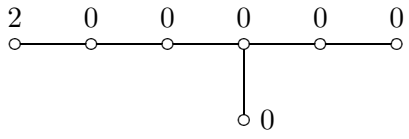
A_2	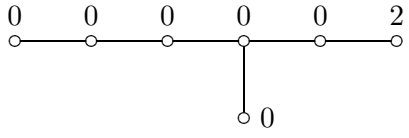
$2A_2$	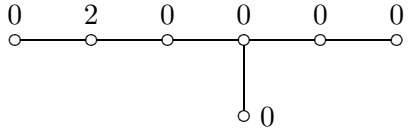
D_4	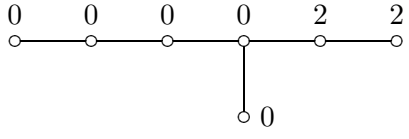
$A_3 + A_2 + A_1$	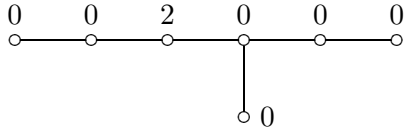

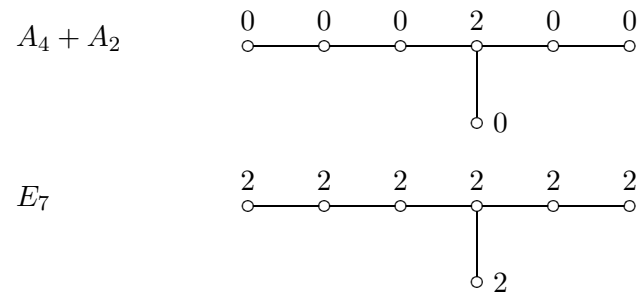

The Satake diagrams $S_{\mathfrak{g}}$ and $\Psi(\mathfrak{b})$ of non-compact real forms $\mathfrak{g}$ of $\mathfrak{g}_{\mathbb{C}}$ are listed in Table 3.7.2 below.

Table 3.7.2. List of Satake diagrams and $\Psi(\mathfrak{b})$ of type E_7.

$\mathfrak{g}$	$S_{\mathfrak{g}}$	$\Psi(\mathfrak{b})$
$\mathfrak{e}_{7(7)}$	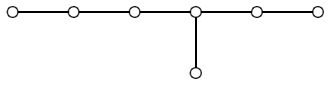	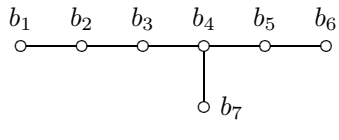
$\mathfrak{e}_{7(-5)}$	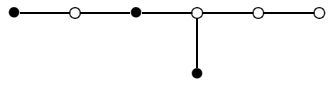	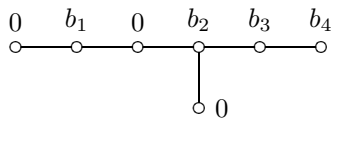
$\mathfrak{e}_{7(-25)}$	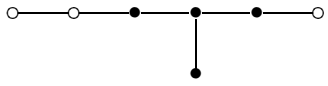	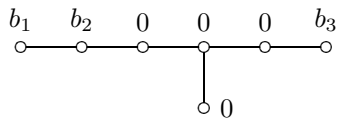

Therefore for each $\mathfrak{g}$, we can find a basis of $\Psi(\mathfrak{b})$ by taking some weighted Dynkin diagrams in $\Psi(\mathcal{H}^n(\mathfrak{a}_+)) = \{\Psi_A \in \Psi(\mathcal{H}^n(\mathfrak{j}_+)) \mid \Psi_A \text{ matches } S_{\mathfrak{g}}\}$ in Table 3.7.3 below.

Table 3.7.3. Examples of bases of $\Psi(\mathfrak{b})$ for real forms of type E_7.

$\mathfrak{g}$	Example of a basis of $\Psi(\mathfrak{b})$
$\mathfrak{e}_{7(7)}$	$3A_1'', A_2, 2A_2, D_4, A_3+A_2+A_1, A_4+A_2, E_7$
$\mathfrak{e}_{7(-5)}$	$A_2, 2A_2, D_4, A_4+A_2$
$\mathfrak{e}_{7(-25)}$	$3A_1'', A_2, 2A_2$

3.8. Type E_8

Let us consider the case where $\mathfrak{g}_{\mathbb{C}}$ is of type E_8, that is, $\mathfrak{g}_{\mathbb{C}} \simeq \mathfrak{e}_{8,\mathbb{C}}$. Then we have

$$\mathrm{Map}(\Pi,\mathbb{R})^{\iota} = \mathrm{Map}(\Pi,\mathbb{R}) = \left\{ \right.$$

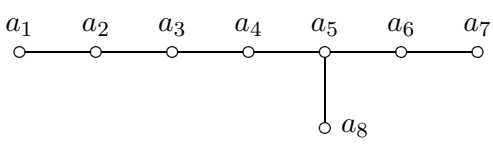

$$\left. \right\}$$

In [4, Section 8.4], we can find some examples of weighted Dynkin diagrams in $\Psi(\mathcal{H}^n(\mathfrak{j}_+))$ as in Table 3.8.1 below.

Table 3.8.1. Examples of weighted Dynkin diagrams in $\Psi(\mathcal{H}^n(\mathfrak{j}_+))$ of type E_8.

Symbol	Weighted Dynkin diagram in $\Psi(\mathcal{H}^n(\mathfrak{j}_+))$
A_2	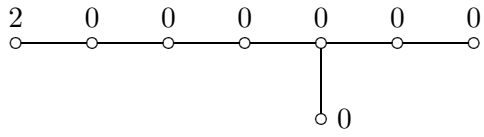
$2A_2$	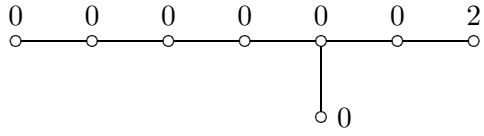

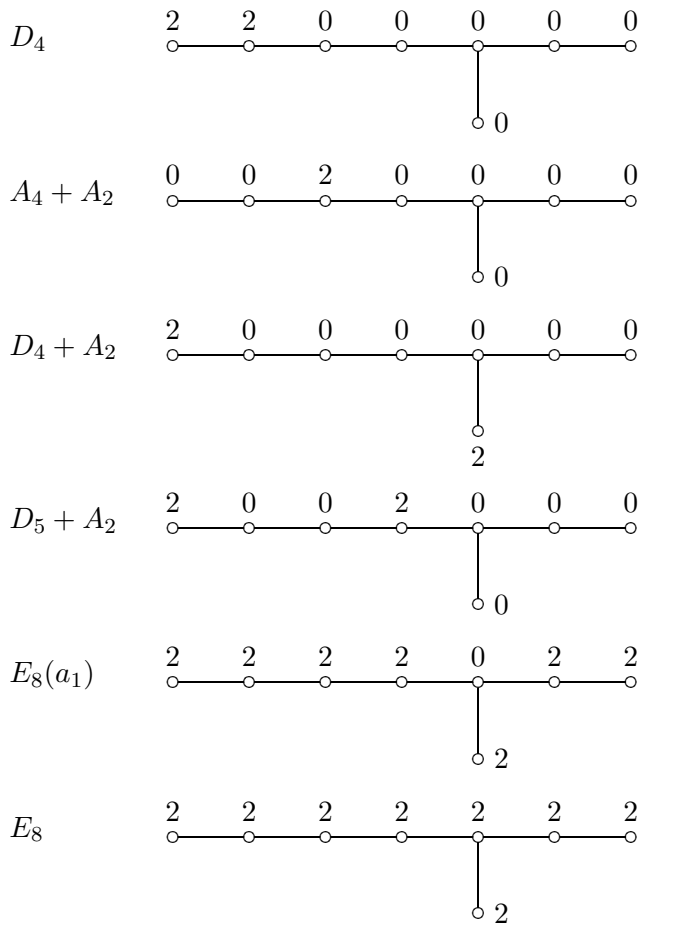

The Satake diagrams $S_{\mathfrak{g}}$ and $\Psi(\mathfrak{b})$ of non-compact real forms $\mathfrak{g}$ of $\mathfrak{g}_{\mathbb{C}}$ are listed in Table 3.8.2 below.

Table 3.8.2. List of Satake diagrams and $\Psi(\mathfrak{b})$ of type E_8.

$\mathfrak{g}$	$S_{\mathfrak{g}}$	$\Psi(\mathfrak{b})$
$\mathfrak{e}_{8(8)}$	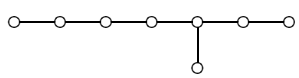	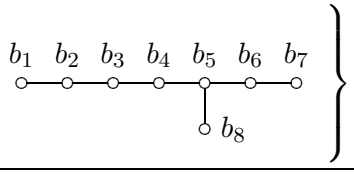

$\mathfrak{e}_{8(-24)}$	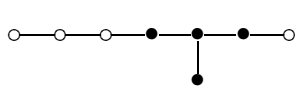	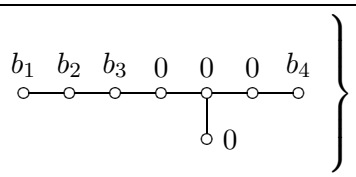

Therefore for each $\mathfrak{g}$, we can find a basis of $\Psi(\mathfrak{b})$ by taking some weighted Dynkin diagrams in $\Psi(\mathcal{H}^n(\mathfrak{a}_+)) = \{\Psi_A \in \Psi(\mathcal{H}^n(\mathfrak{j}_+)) \mid \Psi_A \text{ matches } S_{\mathfrak{g}}\}$ as in Table 3.8.3 below.

Table 3.8.3. Examples of bases of $\Psi(\mathfrak{b})$ for real forms of type E_8.

$\mathfrak{g}$	Example of a basis of $\Psi(\mathfrak{b})$
$\mathfrak{e}_{8(8)}$	$A_2, 2A_2, D_4, A_4+A_2, D_4+A_2, D_5+A_2, E_8(a_1), E_8$
$\mathfrak{e}_{8(-24)}$	$A_2, 2A_2, D_4, A_4+A_2$

3.9. Type F_4

Let us consider the case where $\mathfrak{g}_{\mathbb{C}}$ is of type F_4, that is, $\mathfrak{g}_{\mathbb{C}} \simeq \mathfrak{f}_{4,\mathbb{C}}$. Then we have

$$\mathrm{Map}(\Pi, \mathbb{R})^{\iota} = \mathrm{Map}(\Pi, \mathbb{R}) = \left\{ \begin{array}{c} a_1 \quad a_2 \quad a_3 \quad a_4 \\ \circ\!\!-\!\!\!-\!\!\circ\!\!\Rightarrow\!\!\circ\!\!-\!\!\!-\!\!\circ \end{array} \right\}$$

In [4, Section 8.4], we can find some examples of weighted Dynkin diagrams in $\Psi(\mathcal{H}^n(\mathfrak{j}_+))$ as in Table 3.9.1 below.

Table 3.9.1. Examples of weighted Dynkin diagrams in $\Psi(\mathcal{H}^n(\mathfrak{j}_+))$ of type F_4.

Symbol	Weighted Dynkin diagram in $\Psi(\mathcal{H}^n(\mathfrak{j}_+))$
A_2	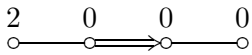

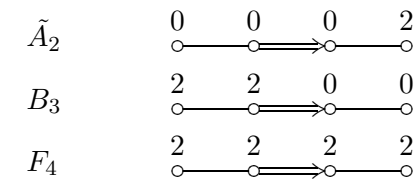

The Satake diagrams $S_{\mathfrak{g}}$ and $\Psi(\mathfrak{b})$ of non-compact real forms $\mathfrak{g}$ of $\mathfrak{g}_{\mathbb{C}}$ are listed in Table 3.9.2 below.

Table 3.9.2. List of Satake diagrams and $\Psi(\mathfrak{b})$ of type F_4.

$\mathfrak{g}$	$S_{\mathfrak{g}}$	$\Psi(\mathfrak{b})$
$\mathfrak{f}_{4(4)}$	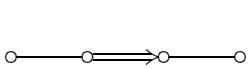	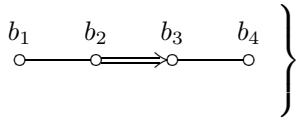
$\mathfrak{f}_{4(-20)}$	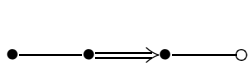	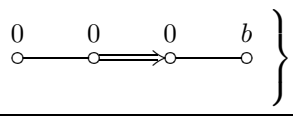

Therefore for each $\mathfrak{g}$, we can find a basis of $\Psi(\mathfrak{b})$ by taking some weighted Dynkin diagrams in $\Psi(\mathcal{H}^n(\mathfrak{a}_+)) = \{\Psi_A \in \Psi(\mathcal{H}^n(\mathfrak{j}_+)) \mid \Psi_A \text{ matches } S_{\mathfrak{g}}\}$ as in Table 3.9.3 below.

Table 3.9.3. Examples of bases of $\Psi(\mathfrak{b})$ for real forms of type F_4.

$\mathfrak{g}$	Example of a basis of $\Psi(\mathfrak{b})$
$\mathfrak{f}_{4(4)}$	$A_2, \tilde{A}_2, B_3, F_4$
$\mathfrak{f}_{4(-20)}$	$\tilde{A}_2$

3.10. Type G_2

Let us consider the case where $\mathfrak{g}_{\mathbb{C}}$ is of type G_2, that is, $\mathfrak{g}_{\mathbb{C}} \simeq \mathfrak{g}_{2,\mathbb{C}}$. Then we have

$$\mathrm{Map}(\Pi, \mathbb{R})^{\iota} = \mathrm{Map}(\Pi, \mathbb{R}) = \left\{ \begin{array}{c} \overset{a_1}{\circ} \Longrightarrow \overset{a_2}{\circ} \end{array} \right\}$$

In [4, Section 8.4], we can find some examples of weighted Dynkin diagrams in $\mathcal{H}^n(\mathfrak{j}_+)$ as in Table 3.10.1 below.

Table 3.10.1. Examples of weighted Dynkin diagrams in $\Psi(\mathcal{H}^n(\mathfrak{j}_+))$ of type G_2.

Symbol	Weighted Dynkin diagram in $\Psi(\mathcal{H}^n(\mathfrak{j}_+))$
$G_2(a_1)$	$\overset{2}{\circ} \Longrightarrow \overset{0}{\circ}$
G_2	$\overset{2}{\circ} \Longrightarrow \overset{2}{\circ}$

Let $\mathfrak{g}$ be a non-compact real form of $\mathfrak{g}_{\mathbb{C}}$. Then $\mathfrak{g}$ is a split real form of $\mathfrak{g}_{\mathbb{C}}$. The Satake diagram $S_{\mathfrak{g}}$ and $\Psi(\mathfrak{b})$ of $\mathfrak{g}$ are listed in Table 3.10.2 below.

Table 3.10.2. List of Satake diagrams and $\Psi(\mathfrak{b})$ of type G_2.

$\mathfrak{g}$	$S_{\mathfrak{g}}$	$\Psi(\mathfrak{b})$
$\mathfrak{g}_{2(2)}$	$\circ \Longrightarrow \circ$	$\left\{ \begin{array}{c} \overset{b_1}{\circ} \Longrightarrow \overset{b_2}{\circ} \end{array} \right\}$

Therefore, the weighted Dynkin diagrams labeled by "$G_2(a_1)$" and "G_2" in $\Psi(\mathcal{H}^n(\mathfrak{a}_+)) = \{\Psi_A \in \Psi(\mathcal{H}^n(\mathfrak{j}_+)) \mid \Psi_A \text{ matches } S_{\mathfrak{g}}\}$ give a basis of $\Psi(\mathfrak{b})$.

Appendix A Semisimple Symmetric Spaces with Proper $SL(2,\mathbb{R})$-Actions

In [9, Theorem 1.3], by using the main result (Theorem 1.1) of this paper, Kobayashi's properness criterion [6, Theorem 4.1] and Benoist's results in [3], we proved that the following three conditions on a semisimple symmetric space G/H are equivalent:

(i) G/H admits a proper action of $SL(2,\mathbb{R})$ via G.

(ii) G/H admits discontinuous groups which are not virtually abelian.

(iii) There exists a (complex) nilpotent orbit $\mathcal{O}^{\mathbb{C}}$ in $\mathfrak{g}_{\mathbb{C}} := \mathfrak{g} + \sqrt{-1}\mathfrak{g}$ such that $\mathcal{O}^{\mathbb{C}}$ meets $\mathfrak{g}$ but does not meet the c-dual $\mathfrak{h} + \sqrt{-1}\mathfrak{q}$ of the symmetric pair $(\mathfrak{g},\mathfrak{h})$, where $\mathfrak{g} = \mathfrak{h} + \mathfrak{q}$ is the decomposition of $\mathfrak{g}$ with respect to the involution associated to the symmetric pair $(\mathfrak{g},\mathfrak{h})$.

In particular, if a symmetric space G/H is simply-connected and satisfies the equivalent conditions above, then for any torsion-free discrete subgroup Γ of $SL(2,\mathbb{R})$ (which acts on G/H properly), we obtain a peudo-Riemmanian locally symmetric space $\Gamma\backslash G/H$ with its fundamental group Γ.

In [9, Table 6], we gave a list of symmetric pair $(\mathfrak{g},\mathfrak{h})$ with simple $\mathfrak{g}$ satisfying the condition (iii). Taking this opportunity, we would like to correct some errors of $(\mathfrak{g},\mathfrak{h})$ in [9, Table 6]:

- "$(\mathfrak{sl}(n,\mathbb{R}),\mathfrak{so}(n-i,i))$ for $2i < n$" should be "$(\mathfrak{sl}(n,\mathbb{R}),\mathfrak{so}(n-i,i))$ for $2i < n-1$".
- "$(\mathfrak{su}(2m-1,2m-1),\mathfrak{so}^*(4m-2))$" should be "$(\mathfrak{su}(n,n),\mathfrak{so}^*(2n))$".
- "$(\mathfrak{so}(k,k),\mathfrak{so}(2k,\mathbb{C})+\mathfrak{so}(2))$" should be "$(\mathfrak{so}(k,k),\mathfrak{so}(k,\mathbb{C})+\mathfrak{so}(2))$".
- "$(\mathfrak{sl}(n,\mathbb{C}),\mathfrak{so}(n-i,i))$ for $2i < n$" should be "$(\mathfrak{sl}(n,\mathbb{C}),\mathfrak{so}(n-i,i))$ for $2i < n-1$".

For the reader's convenience we give a list of symmetric pair $(\mathfrak{g},\mathfrak{h})$ with simple $\mathfrak{g}$ satisfying the condition (iii) as Table A below.

Table A. Classification of $(\mathfrak{g}, \mathfrak{h})$ satisfying the condition $(\star)$.

$\mathfrak{g}$	$\mathfrak{h}$
$\mathfrak{sl}(2k, \mathbb{R})$	$\mathfrak{sl}(k, \mathbb{C}) \oplus \mathfrak{so}(2)$
$\mathfrak{sl}(n, \mathbb{R})$	$\mathfrak{so}(n-i, i)$ $(2i < n-1)$
$\mathfrak{su}^*(2k)$	$\mathfrak{sp}(k-i, i)$ $(2i < k-1)$
$\mathfrak{su}(2p, 2q)$	$\mathfrak{sp}(p, q)$
$\mathfrak{su}(n, n)$	$\mathfrak{so}^*(2n)$
$\mathfrak{su}(p, q)$	$\mathfrak{su}(i, j) \oplus \mathfrak{su}(p-i, q-j) \oplus \mathfrak{so}(2)$ $(\min\{p, q\} > \min\{i, j\} + \min\{p-i, q-j\})$
$\mathfrak{so}(p, q)$ ($p+q$ is odd)	$\mathfrak{so}(i, j) \oplus \mathfrak{so}(p-i, q-j)$ $(\min\{p, q\} > \min\{i, j\} + \min\{p-i, q-j\})$
$\mathfrak{sp}(n, \mathbb{R})$	$\mathfrak{su}(n-i, i) \oplus \mathfrak{so}(2)$
$\mathfrak{sp}(2k, \mathbb{R})$	$\mathfrak{sp}(k, \mathbb{C})$
$\mathfrak{sp}(p, q)$	$\mathfrak{sp}(i, j) \oplus \mathfrak{sp}(p-i, q-j)$ $(\min\{p, q\} > \min\{i, j\} + \min\{p-i, q-j\})$
$\mathfrak{so}(p, q)$ ($p+q$ is even)	$\mathfrak{so}(i, j) \oplus \mathfrak{so}(p-i, q-j)$ $(\min\{p, q\} > \min\{i, j\} + \min\{p-i, q-j\},$ unless $p = q = 2m+1$ and $\lvert i-j \rvert = 1)$
$\mathfrak{so}(2p, 2q)$	$\mathfrak{su}(p, q) \oplus \mathfrak{so}(2)$
$\mathfrak{so}^*(2k)$	$\mathfrak{su}(k-i, i) \oplus \mathfrak{so}(2)$ $(2i < k-1)$
$\mathfrak{so}(k, k)$	$\mathfrak{so}(k, \mathbb{C}) \oplus \mathfrak{so}(2)$
$\mathfrak{so}^*(4m)$	$\mathfrak{so}^*(4m-4i+2) \oplus \mathfrak{so}^*(4i-2)$
$\mathfrak{e}_{6(6)}$	$\mathfrak{sp}(2, 2)$
$\mathfrak{e}_{6(6)}$	$\mathfrak{su}^*(6) \oplus \mathfrak{su}(2)$
$\mathfrak{e}_{6(2)}$	$\mathfrak{so}^*(10) \oplus \mathfrak{so}(2)$
$\mathfrak{e}_{6(2)}$	$\mathfrak{su}(4, 2) \oplus \mathfrak{su}(2)$
$\mathfrak{e}_{6(2)}$	$\mathfrak{sp}(3, 1)$
$\mathfrak{e}_{6(-14)}$	$\mathfrak{f}_{4(-20)}$
$\mathfrak{e}_{7(7)}$	$\mathfrak{e}_{6(2)} \oplus \mathfrak{so}(2)$
$\mathfrak{e}_{7(7)}$	$\mathfrak{su}(4, 4)$
$\mathfrak{e}_{7(7)}$	$\mathfrak{so}^*(12) \oplus \mathfrak{su}(2)$

$\mathfrak{e}_{7(7)}$	$\mathfrak{su}^*(8)$
$\mathfrak{e}_{7(-5)}$	$\mathfrak{e}_{6(-14)} \oplus \mathfrak{so}(2)$
$\mathfrak{e}_{7(-5)}$	$\mathfrak{su}(6,2)$
$\mathfrak{e}_{7(-25)}$	$\mathfrak{e}_{6(-14)} \oplus \mathfrak{so}(2)$
$\mathfrak{e}_{7(-25)}$	$\mathfrak{su}(6,2)$
$\mathfrak{e}_{8(8)}$	$\mathfrak{e}_{7(-5)} \oplus \mathfrak{su}(2)$
$\mathfrak{e}_{8(8)}$	$\mathfrak{so}^*(16)$
$\mathfrak{f}_{4(4)}$	$\mathfrak{sp}(2,1) \oplus \mathfrak{su}(2)$
$\mathfrak{sl}(2k,\mathbb{C})$	$\mathfrak{su}^*(2k)$
$\mathfrak{sl}(n,\mathbb{C})$	$\mathfrak{su}(n-i,i)$ $(2i < n-1)$
$\mathfrak{so}(2k+1,\mathbb{C})$	$\mathfrak{so}(2k+1-i,i)$ $(i < k)$
$\mathfrak{sp}(n,\mathbb{C})$	$\mathfrak{sp}(n-i,i)$
$\mathfrak{so}(2k,\mathbb{C})$	$\mathfrak{so}(2k-i,i)$ $(i < k$ unless $k = i+1 = 2m+1)$
$\mathfrak{so}(4m,\mathbb{C})$	$\mathfrak{so}(4m-2i+1,\mathbb{C}) \oplus \mathfrak{so}(2i-1,\mathbb{C})$
$\mathfrak{so}(2k,\mathbb{C})$	$\mathfrak{so}^*(2k)$
$\mathfrak{e}_{6,\mathbb{C}}$	$\mathfrak{e}_{6(-14)}$
$\mathfrak{e}_{6,\mathbb{C}}$	$\mathfrak{e}_{6(-26)}$
$\mathfrak{e}_{7,\mathbb{C}}$	$\mathfrak{e}_{7(-5)}$
$\mathfrak{e}_{7,\mathbb{C}}$	$\mathfrak{e}_{7(-25)}$
$\mathfrak{e}_{8,\mathbb{C}}$	$\mathfrak{e}_{8(-24)}$
$\mathfrak{f}_{4,\mathbb{C}}$	$\mathfrak{f}_{4(-20)}$

Here $k \geq 1$, $m \geq 1$, $n \geq 2$, $p, q \geq 1$ and $i, j \geq 0$. It should be remarked that $\mathfrak{so}(p,q)$ is simple if and only if $p+q \geq 3$ and $(p,q) \neq (2,2)$, $\mathfrak{so}(2k,\mathbb{C})$ is simple if and only if $k \geq 3$.

Acknowledgements. The author would like to give warm thanks to Toshiyuki Kobayashi and Hiroyuki Ochiai whose comments were of inestimable value for this paper. The author also thanks Yosuke Morita and Koichi Tojo for pointing out some errors in [9, Table 6]. This work is supported by JSPS KAKENHI Grant Number JP16K17594.

References

[1] Araki, S., On root systems and an infinitesimal classification of irreducible symmetric spaces, J. Math. Osaka City Univ. **13** (1962), 1–34.

[2] Bala, P. and R. W. Carter, Classes of unipotent elements in simple algebraic groups. I, II, Math. Proc. Cambridge Philos. Soc. **79** (1976), 401–425; *bid* **80** (1976), 1–17.

[3] Benoist, Y., Actions propres sur les espaces homogènes réductifs, Ann. of Math. (2) **144** (1996), 315–347.

[4] Collingwood, D. H. and W. M. McGovern, *Nilpotent orbits in semisimple Lie algebras*, Van Nostrand Reinhold Mathematics Series, Van Nostrand Reinhold Co., New York, 1993.

[5] Dynkin, E. B., Semisimple subalgebras of semisimple Lie algebras, Amer. Math. Soc. Transl. **6** (1957), 111–244.

[6] Kobayashi, T., Proper action on a homogeneous space of reductive type, Math. Ann. **285** (1989), 249–263.

[7] Kostant, B., The principal three-dimensional subgroup and the Betti numbers of a complex simple Lie group, Amer. J. Math. **81** (1959), 973–1032.

[8] Malcev, A. I., On semi-simple subgroups of Lie groups, Amer. Math. Soc. Translation **1950** (1950), 43 pages.

[9] Okuda, T., Classification of semisimple symmetric spaces with proper $SL(2,\mathbb{R})$-actions, J. Differential Geom. **94** (2013), 301–342.

[10] Satake, I., On representations and compactifications of symmetric Riemannian spaces, Ann. of Math. **71** (1960), 77–110.

[11] Tits, J., *Classification of algebraic semisimple groups*, Algebraic Groups and Discontinuous Subgroups (Proc. Sympos. Pure Math., Boulder, Colo., 1965), Amer. Math. Soc., (1966), 33–62.

(Received December 9, 2016)

Department of Mathematics
Graduate School of Science
Hiroshima University
1-3-1 Kagamiyama
Higashi-Hiroshima, 739-8526 Japan
E-mail: okudatak@hiroshima-u.ac.jp